Electronic Supplementary Material (ESI) for Dalton Transactions.
This journal is © The Royal Society of Chemistry 2022

Supplemental Material

Toward controlling the Al_2O_3/ZnO interface properties by *in-situ* ALD preparation

Christoph Janowitz,[a] Ali Mahmoodinezhad,[a] Małgorzata Kot,[a] Carlos Morales,[a] Franziska Naumann,[b] Paul Plate,[b] Marvin Hartwig Zoellner,[c] Florian Bärwolf,[c] Dawid Stolarek,[c] Christian Wenger,[c] Karsten Henkel,[a] and Jan Ingo Flege[a]*

[a]Applied Physics and Semiconductor Spectroscopy, Brandenburg University of Technology Cottbus–Senftenberg, K.-Zuse-Str. 1, 03046 Cottbus, Germany
[b]SENTECH Instruments GmbH, Schwarzschildstraße 2, 12489 Berlin, Germany
[c]IHP – Leibniz-Institut für innovative Mikroelektronik, Im Technologiepark 25, 15236 Frankfurt (Oder), Germany

1) Ellipsometry:

Routinely, ellipsometry data of the ALD layers were measured after ALD preparation. Thicknesses of 10.20 nm ± 0.85 nm and 59.40 nm ± 0.65 nm were obtained for the PEALD-Al_2O_3 and TALD-ZnO layers, which were deposited across 4-inch silicon wafers (cf. Fig. S1). The ZnO and Al_2O_3 ellipsometric parameters were fitted simultaneously. The map in Fig. S1 summarizes 69 measurements across the 4-inch wafer corroborating its thickness homogeneity.

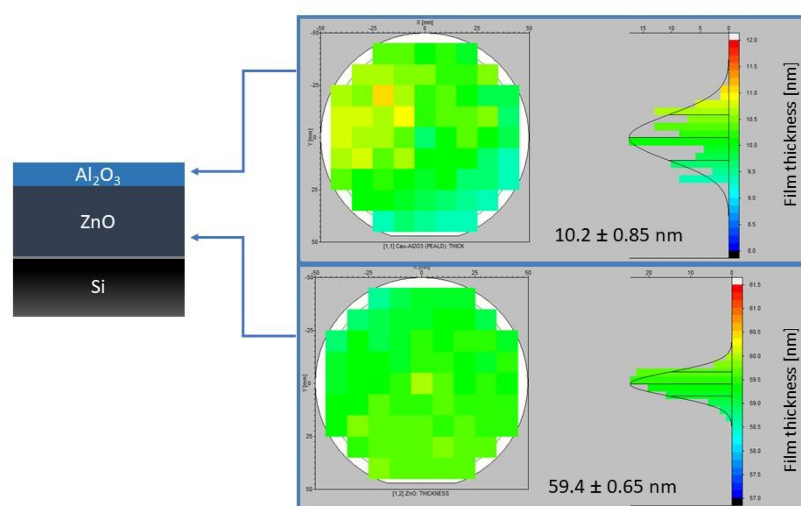

FIG. S1: 4-inch map of the Al_2O_3 (upper part) and ZnO (lower part) film thicknesses from simultaneous fitting of ellipsometric parameters of these layers. Here results of the "10 nm PEALD-Al_2O_3 on 59 nm TALD-ZnO" wafer are shown.

Similar results were also recorded for other wafers investigated, including (i) "10 nm TALD-Al_2O_3 on 59 nm TALD-ZnO"; (ii) "3 nm PEALD-Al_2O_3 on 59 nm TALD-ZnO"; and (iii) "3 nm TALD-Al_2O_3 on 59 nm TALD-ZnO". These values were confirmed by

X-ray reflectometry (XRR, data not shown) and scanning electron microscopy (SEM, see below) measurements.

2) Grazing-Incidence X-ray Diffraction: (GIXRD)

To determine the crystallographic structure and thickness, grazing-incidence X-ray diffraction (GIXRD) and XRR have been applied. For this purpose, a Rigaku SmartLab comprising a 9 kW rotating Cu anode with line focus has been used. The incident beam was monochromatized with a 2-bounce Ge(400) channel-cut crystal. The sample was aligned with respect to the total reflection. During GIXRD measurements, the incidence angle α was set to 0.5°, while 2Θ was scanned from 20-70°.

As mentioned in the previous section, the interference fringes in the XRR data are in agreement with the thicknesses determined by ellipsometry.

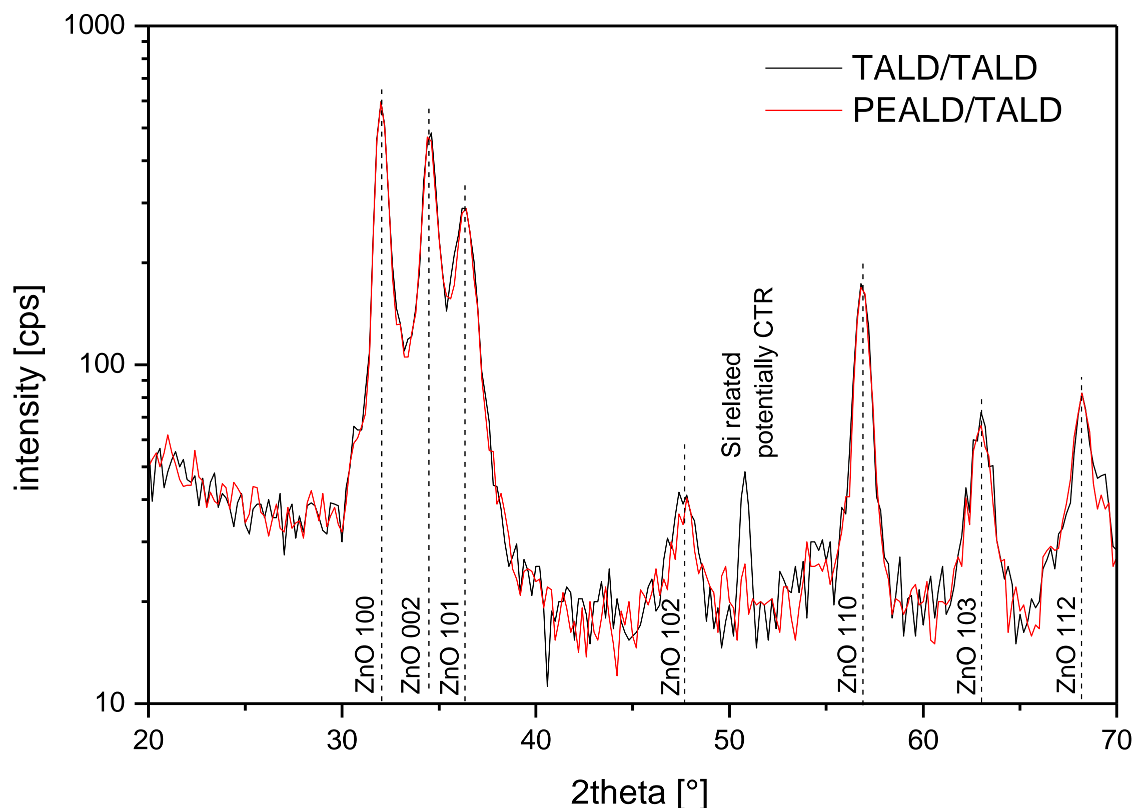

FIG. S2: GIXRD patterns of the samples “10 nm PEALD-Al_2O_3 on 59 nm TALD-ZnO” (PEALD/TALD, red line) and “10 nm TALD-Al_2O_3 on 59 nm TALD-ZnO” (TALD/TALD black line).

The GIXRD patterns of the samples (i) “10 nm PEALD-Al_2O_3 on 59 nm TALD-ZnO” and (ii) “10 nm TALD-Al_2O_3 on 59 nm TALD-ZnO” are shown in Fig. S2. In both cases, when rotating the sample around the normal, a diffraction pattern attributable solely to ZnO clearly appeared. In contrast, no indication for crystalline Al_2O_3 is present. Also a feature from the underlying Si substrate is observed, which is probably due to some crystal truncation rod (CTR) as it varies with the rotation of the sample. Typically, this feature was also observed on different samples.

We conclude that for both samples the Al_2O_3 film is amorphous whereas the ZnO layer is polycrystalline. Similar results were obtained in /Chaaya et al., *J. Phys. Chem. C* 118, 3811 (2014)/ for a purely TALD-grown interface.

3) Scanning Electron Microscopy

SEM images of the layer stacks were recorded using a Zeiss Gemini 2 tool.

The image of the cross section of the “10 nm PEALD-Al_2O_3 on 59 nm TALD-ZnO” sample confirms the layer thickness of the ellipsometric and XRR measurements and depicts an abrupt interface within the resolution of the instrument (Fig. S3). The picture taken on top of the Al_2O_3 layer shows a uniform surface with randomly oriented structures of ellipsoidal shape, whose length does not exceed 80 nm (Fig. S4). Considering the XRD data, these features belong to ZnO while the amorphous Al_2O_3 conformally covers the polycrystalline ZnO structures.

Similar results were obtained for the “10 nm TALD-Al_2O_3 on 59 nm TALD-ZnO” sample.

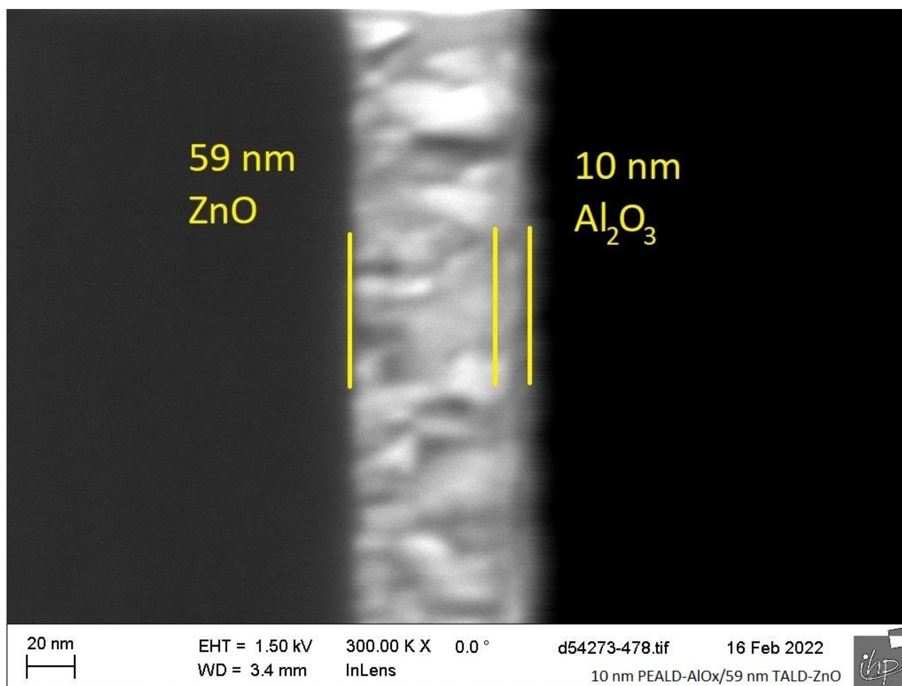

FIG. S3. SEM image of the interface region (cross section) of the “10 nm PEALD-Al_2O_3 on 59 nm TALD-ZnO” sample.

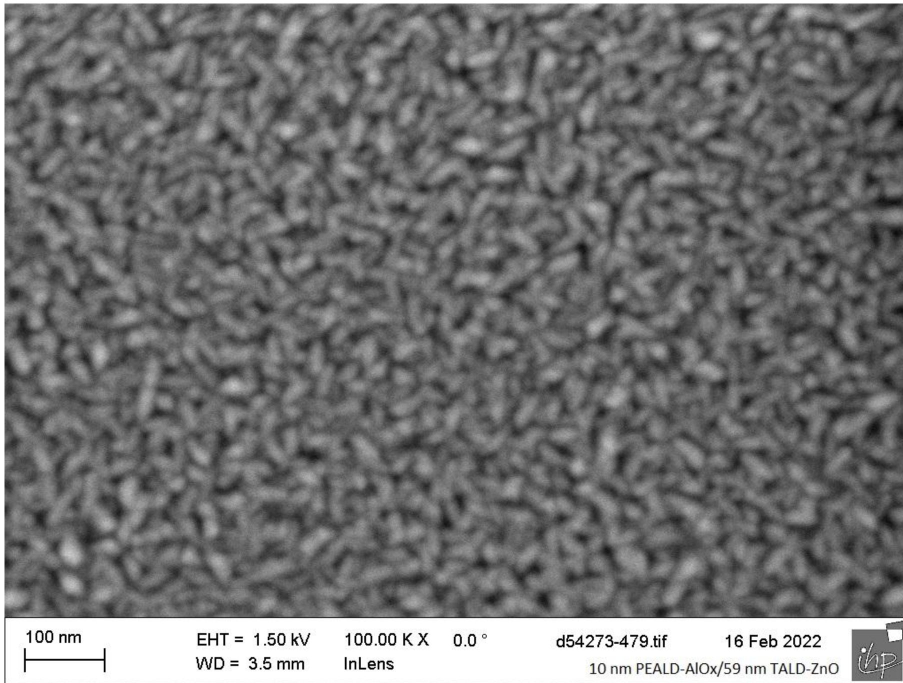

FIG. S4. SEM image of the surface of the “10 nm PEALD-Al_2O_3 on 59 nm TALD-ZnO” sample.

4) X-ray Photoelectron Spectroscopy (XPS):

Here, we include the Al 2p spectra from the sample “10 nm PEALD-Al_2O_3 on 59 nm TALD-ZnO” reported in the manuscript (Fig. S5).

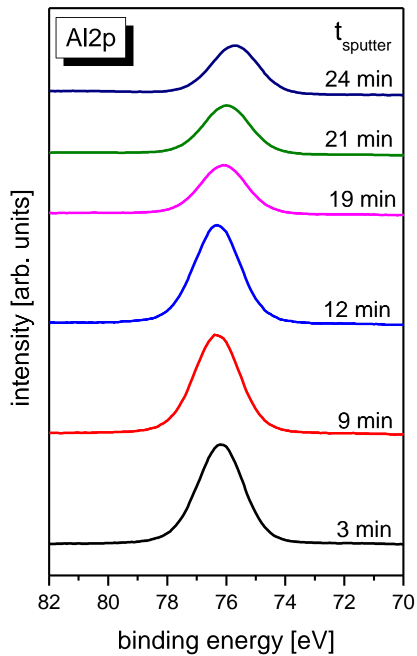

FIG. S5: Depth profiling in terms of the Al 2p XPS core level of the “10 nm PEALD-Al_2O_3 on 59 nm TALD-ZnO” sample.

It is obvious that the peak does not change its shape with sputter time. It can well be fitted by a single Voigt profile of 1.67 ± 0.10 eV widths (full width at half maximum). In principle, the broadened overall peak shape could comprise several small additional components, but their absolute intensity is weak and does not change significantly with sputter time. However, an upward band bending with increasing sputter time is clearly evident.

In addition, we performed measurements on a sample with only 3 nm PEALD-Al_2O_3 on top of 59 nm TALD-ZnO using besides Mg Kα also Al Kα excitation (more bulk sensitive than Mg Kα) to ensure a non-destructive XPS characterization of the Al_2O_3/ZnO interface.

In particular, the Zn 2p core level of the as-inserted sample taken with Al Kα showed a shoulder on the low binding energy side, corresponding to a splitting due to Zn-Zn and ZnO in the interface region. After extended sputtering, the ZnO showed just a single Zn 2p peak due to ZnO bonds. These data confirm the data shown in Fig. 7 of the manuscript.

We also recorded Zn L_3MM Auger data for the non-sputtered sample and after 5 min of sputtering (Fig. S6). The line shape of the non-sputtered sample (corresponding to the interface region for this sample with the thinner Al_2O_3 on top) resembled the situation of a mix of Zn-O and Zn-Zn bonds, whereas the data after 5 min sputtering reflect the situation of solely Zn-O bonds.

Overall, these data confirm the XPS findings presented in the manuscript regarding the formation of Zn-Zn bonds at the interface of our ALD-prepared Al_2O_3/ZnO heterojunction and negate the possibility that this behavior is just a sputter artifact.

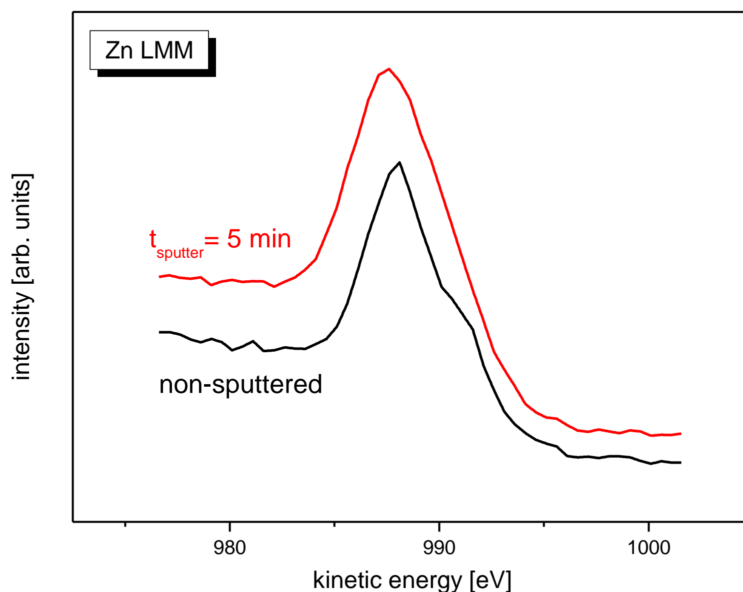

FIG. S6 Zn L_3MM Auger data recorded following bulk sensitive Al Kα excitation on a "3 nm PEALD-Al_2O_3 on 59 nm TALD-ZnO" sample.